

GENERATION OF RUNAWAY ELECTRON BEAMS AND USE OF THESE BEAMS FOR PUMPING METAL VAPOR LASERS

G.V. Kolbychev

*Institute of Atmospheric Optics,
Siberian Branch of the Russian Academy of Sciences, Tomsk
Received March 17, 1993*

An efficient way of generating 2-10 keV electron beams in a medium-pressure pulsed gas discharge is described. A detailed description of the generation process is also given. A relationship of the beam generation efficiency with the length of the interelectrode gap and the intensity of an external UV illumination has been established. It is shown that under optimal generation conditions the cathode-fall region is abnormally large and fills up the whole discharge gap. Different versions of using these beams for pumping the metal vapor lasers are discussed, which provide efficiency of pumping being an order of magnitude higher as compared to the pulsed discharge pumping. For a radial arrangement of pumping the input energy can reach from 10 to 20 J/m per pulse. For a longitudinal arrangement of pumping the operation at a pulse repetition rate of several hundreds of kilohertz with an average input power of about 50 kW per every 10s Hz is possible without a decrease in the overall efficiency of the laser. Advantages and drawbacks of both versions of pumping are determined and some physical and technical limitations on the beam and laser parameters are revealed.

1. INTRODUCTION

In the 80s, an efficient method for producing pulsed electron beams immediately in a medium-pressure gas discharge was developed.¹⁻³ Thus, the main obstacle for using e-beams in lasers consisting in the necessity of mounting a thin foil between the operating cavity of the electron gun and the laser cell was eliminated. Additional advantages of the new e-guns over conventional electron generators are their versatile operating capabilities, compactness and compatibility with standard power supplies. The interest in the guns is quite natural owing to their good performance, serviceability, as well as the ways they are used.

So far the information about the new guns has been drawn mainly from papers of Bokhan and the author of this article (see list of references), which, of course, give but a rough idea about the subject under consideration. Moreover, Bokhan and I have a different insight into the physical mechanism of e-beam generation, mechanism of the discharge and its instabilities, and ways of solving the technical problems. Thus, the situation is considerably challenging for understanding by other researchers.

In this paper the available data concerning the e-beam production by this method, e-beam characteristics, and use of the e-beam for metal vapor laser excitation are analyzed.

2. A WAY OF GENERATION OF RUNAWAY ELECTRON BEAMS

The e-beam is produced in a pulsed space discharge initiated in a narrow gas gap between a solid cold cathode and a grid anode.¹⁻³ A simplified circuit diagram of the e-beam generator and wave forms of the cathode voltage U_d , anode current I_a , and e-beam current I_e onto the collector CF are shown in Fig. 1. Typical initial parameters are as follows: the interelectrode distance $d = 0.2-1$ mm, the drift space length between the anode

and the collector CF $L \geq 25$ mm, the power supply voltage $U_0 = 4-10$ kV, and the discharge capacitance per unit of the cathode effective area $C_d = 0.1-1$ nF/cm².

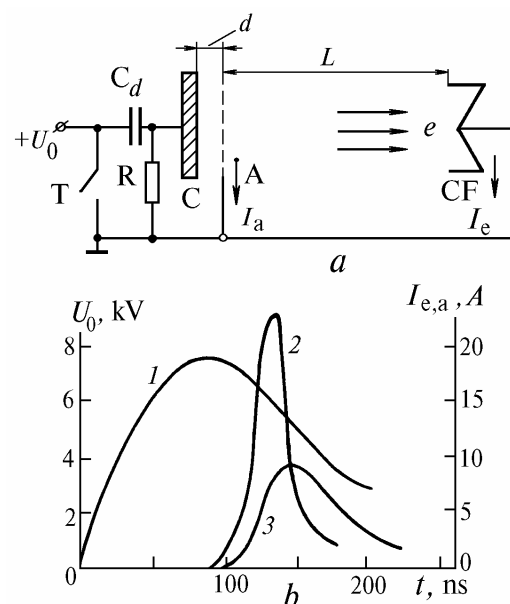


FIG. 1. The runaway electron gun: a) schematic diagram and b) wave forms of cathode voltage (1), e-beam current onto the collector (2), and current flowing in the anode circuit (3). $d = 0.5$ mm, $P_{He} = 4$ kPa, and cathode area $S_c = 0.8$ cm².

Shown in Fig. 2 are the wave forms of U_d and I_a and peak values of I_a and I_e as a function of power supply voltage U_0 . It should be noted that with varying the supply voltage, type, and pressure of a gas the e-beam current density and

FWHM width vary in the ranges 0.1–100 A/cm² and 10–10⁴ ns, respectively. Usually, the number of electrons per pulse extracted per unit area from the cathode

does not exceed 1 · 10¹³ cm⁻², but in some experiments it reaches (3–5) · 10¹³ cm⁻². This parameter is determined mainly by the voltage U₀ and depends weakly on the gas pressure.

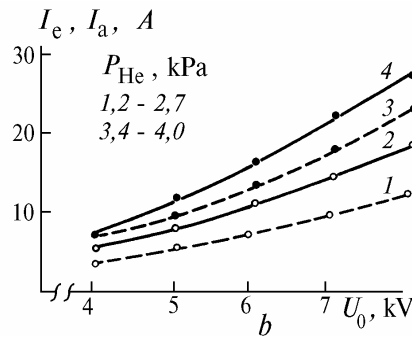
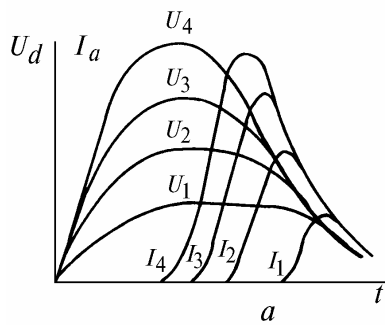


FIG. 2. Waveforms of cathode voltage U_{1–4} and anode current I_{1–4} vs the power supply voltage increasing with subscript number (a) and e-beam current pulse amplitude (2, 4) and anode current (1, 3) vs the power supply voltage U₀(b). d = 05 mm and S_c = 0.8 cm².

The average beam electron energy is defined as $\bar{\varepsilon} \approx e \cdot U_{e/\max}$, where U_{e/max} is the voltage across the gap at the instant when the e-beam current reaches its peak value. As a rule, we have U_{e/max} = (0.7–0.8) · U₀ (see Ref. 4).

For a weakly ionized gas (E/N)_{thr} is determined by the formula^{2,7}

The discharge development and the e-beam generation are delayed by some hundreds of nanoseconds from the instant of application of voltage to the gap. Owing to this fact, the requirements to the switch T which is usually a hydrogen thyratron are not very stringent.

$$(E/N)_{thr} = 4\pi e^3 Z / (2.72 \varepsilon^*);$$

The efficiency of the e-beam production in a discharge can be estimated by the relation

$$(E/P)_{thr} \approx 2.54 \cdot 10^3 Z / \varepsilon^*, B / (\text{Pa}\cdot\text{m}), \tag{2}$$

$$\eta = \frac{Q_e}{\mu_a(Q_e + Q_a)}, \tag{1}$$

where e and Z are the charges of an electron and a gas particle, ε* is an average excitation energy in eV. The value (E/P)_{thr} is about 50, 90, 230, and 275 V/(Pa·m) for helium, hydrogen, xenon, and nitrogen, respectively.⁸

where Q_e and Q_a are the charges carried during the current pulses I_e and I_a, respectively and μ_a is the geometric transmittance of the anode grid. The efficiency grows with increasing the supply voltage U₀ and equals 60–80% under typical conditions of operation. When the conditions are far from optimal, for example, when U₀ is too low or gas pressure is too high, the efficiency η is as low as 30–40%. Conversely, if the conditions are optimal η can reach ~ 90–95%.

It should be taken into account that in a medium-pressure gas the (E/P)_{thr} value is much higher than it needs for an electrical breakdown of the gas gap. The fast development of the discharge hinders the generation of a high-energy runaway electron beam because of the redistribution of the electric field in the gap and the appearance of a great number of low energy electrons. The efficiency of the e-beam production in this case is estimated as³

The way of the above-described e-beam production shows excellent frequency characteristics. As our examinations show, the e-beam parameters vary only slightly with increasing the pulse repetition rate from 0.5 to 40 kHz. These observations were proceeded in Bokhan's experiments up to the frequencies 300 kHz, and the possibility to generate e-beams with repetition rates of 3 MHz was verified.^{5,6} The high-repetition rate regime of operation is favorable for stabilization of the initiation and development of a space discharge in an interelectrode gap.

$$\eta = \gamma / (1 + \gamma), \tag{3}$$

where γ is the second Townsend coefficient. Under the conditions of a glow discharge since γ ≤ 0.2 (see Ref. 9) we have η ≤ 17%. In all previous experiments (see, e.g., Ref. 10) the value η did not exceed 1–3%.

3. MECHANISM OF THE GENERATION OF RUNAWAY ELECTRON BEAMS

The e-beam production in a medium-pressure gas is a result of the changeover of electrons into a runaway regime of motion in a strong electric field between the cathode and anode. The running away phenomenon is of threshold nature with respect to parameters E/N, where E is the electric field strength and N is the gas density.

The main features of the method described in Sec. 1 that provides the efficiency 60–80% of e-beam production are as follows:

- (i) the application to the gap of a very strong external electric field being at least tenfold higher than the threshold for electron runaway,
- (ii) the existence of an intense UV illumination being external with respect to the gap that provides photoelectron emission from the cathode, and
- (iii) the short interelectrode gap.

Let us consider the effect of these factors on the discharge dynamics and the e-beam production in the gap.

A very strong electric field. Application of an electric field to a gap of length d filled with a gas of density N leads to an appearance of electron avalanches there. When E/N ≫ (E/N)_{thr} each electron in the avalanche is a runaway electron, and as early as on its first free path it acquires a kinetic energy exceeding by an order of magnitude or more the energy it may lose due to its collisions with gas particles. The general equation describing the development of a runaway electron

avalanche is derived elsewhere.¹¹ This equation can be written down with good precision in the form¹²

$$w(x) = \beta N \int_0^x w(\xi) \sigma_i [\varphi(x) - \varphi(\xi)] d\xi \quad (4)$$

with the initial condition $w(0) = \delta(0)$, where $\delta(0)$ is the Dirac delta-function, $w(x)$ is the density of ionization by the runaway electron avalanche at the distance x from the start point of the first initiating electron, β is the average ratio of path length of runaway electron to the drift length along the electric field, $\sigma_i(x, \xi)$ is the gas ionization cross section at the point x for the runaway electron generated at the point ξ , $\varphi(x)$ and $\varphi(\xi)$ are the electric field potentials at the points x and ξ , respectively. The value β in our case is close to unity, since it is about 1.4 even if the applied electric field is comparatively weak 90 V/(Pa·m) (see Ref. 13). According to Eq. (4), the electron current gain in a gas is given in the form

$$K(d) = \int_{0 <}^d w(x) dx. \quad (5)$$

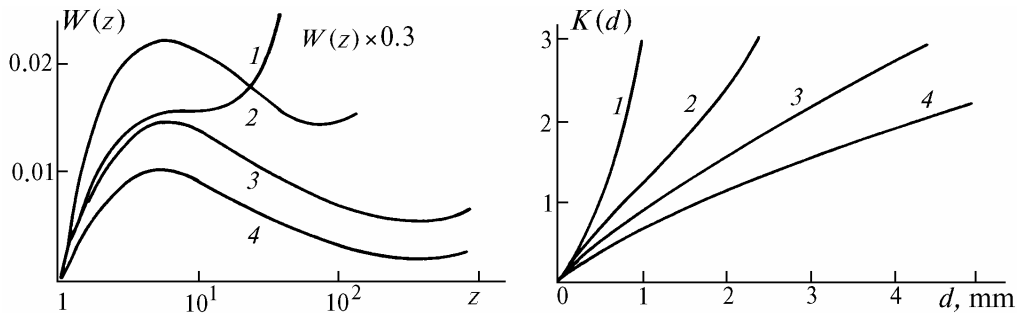


FIG. 3. Plots of the $W(z)$ and $K(d)$ functions for helium at $N = 4 \cdot 10^{23} \text{ m}^{-3}$ and $E = 1$ (1), 2 (2), 3 (3), and 4 (4) · V/m.

An external UV illumination. As early as in the first experiments^{3,11} it was noticed that the e-beam production by the above-described way and the discharge dynamics are strongly affected by the light illumination taking place from the drift space behind the anode (see Fig. 1). The illumination is initiated by the e-beam injected through the grid anode into the gap. As demonstrated in Refs. 11, 15, and 16, the illumination produces an intense flux of photoelectrons from the cathode and increases the efficiency of e-beam production η in the discharge.

Figure 4 shows experimentally obtained dependencies of η on the initial parameters of the gap and the intensity of UV illumination. The latter was varied using attenuators with calibrated geometrical transmittances placed in the drift space. The greater the transmittance, the higher is the illumination intensity.

The effect of the UV illumination can be estimated in the following manner. Let UV photons appear as a result of direct gas particle excitation by an e-beam passing through the drift space. Then the discharge current gain through this mechanism can be represented in the form

$$\begin{aligned} \kappa_V &= \mu_a^2 \gamma_v \int_0^{eU_d} w(\varepsilon) d\varepsilon \int_0^{l_m(\varepsilon)} \Phi(x) \frac{\theta_v}{h\nu} \left(-\frac{d\varepsilon}{dx} \right)_e dx = \\ &= \mu_a^2 \gamma_v \frac{\theta_v}{h\nu} \int_0^{eU_d} w(\varepsilon) d\varepsilon \int_0^\varepsilon \Phi[x(\varepsilon, \varepsilon')] d\varepsilon', \quad (6) \end{aligned}$$

The function $w(x)$ is introduced because the first Townsend coefficient loses its universality under the conditions of electron runaway and the description of gas ionization in terms of this quantity becomes too complicated.

Figure 3 shows the results of numerical calculations of the functions $W(z) = r \cdot w(x)$ by formulas (4) and (5) (where $z = e \cdot \varphi(x) / J$, $r = J / (e \cdot E)$, $x = r \cdot z$, and J is the ionization potential) and $K(d)$ for helium at $\beta = 1$. The cross section σ_i is approximated by Drawin's formula with unit adjusting coefficients. It can be seen from Eqs. (4) and (5) that if $E/N = \text{const}$ then $w(x)$ and $K(d)$ conserve their magnitudes, but the linear coordinate x decreases proportionally with increase of E . Figure 3 shows that the growth of runaway electron avalanches in very strong electric fields at the initial stages of its own development does not obey the well-known exponential Townsend law. But if the electric field is not so strong or the avalanches are far from their start points, then the growth of avalanches approaches asymptotically to this law.¹¹ Note additionally that the recent calculations performed with Monte Carlo code¹⁴ and those performed using Eq. (4) are in a good agreement.

where

$$x(\varepsilon, \varepsilon') = \int_{\varepsilon'}^\varepsilon \frac{d\varepsilon}{(-d\varepsilon/dx)_e} \approx \frac{1}{16\pi e^4 ZN} \left[\frac{\varepsilon^2}{\ln(4\varepsilon/\varepsilon^*)} - \frac{(\varepsilon')^2}{\ln(4\varepsilon'/\varepsilon^*)} \right].$$

Here μ_a is the geometrical transmittance of the anode, γ_v is the coefficient of a photoelectron emission from the cathode, $\Phi(x)$ is the fraction of the UV photons produced at the distance x from the anode which reaches the cathode, $l_m(\varepsilon)$ is the total pathlength of the electron with initial kinetic energy ε , $\overline{h\nu}$ is an average energy of the UV photons, $(-d\varepsilon/dx)_e$ is the e-beam energy lost per unit length in the drift space,¹⁷ and θ_v is the fraction of the e-beam energy expended for production of UV photons. The integrand $w(\varepsilon)$ takes into account the initial energy distribution in the e-beam. Estimation of κ_v for the case of helium for $N = 8 \cdot 10^{23} \text{ m}^{-3}$, $\theta_v = 0.2$, $\overline{h\nu} = 5 \text{ eV}$, $\gamma_v = 0.1$, $\mu_a = 0.8$, $d = 0.5 \text{ mm}$, $U_0 = 6 \text{ kV}$, and a round anode of 1 cm in diameter yields the value $\kappa_v = 2-3$. The greatest contribution to the UV illumination is provided by the beam electrons generated near the anode and having relatively low kinetic energies. The UV illumination effect increases with increasing the anode diameter because the function $\Phi(x)$ depends very strongly on the geometry of the discharge gap.

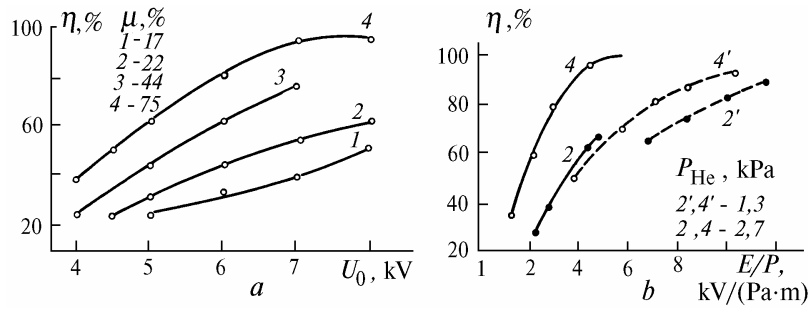


FIG. 4. E-beam production efficiency η vs power supply voltage $U_0(a)$ and parameter E/P (b) for different geometrical transmissivities μ of the UV illumination attenuator.

The above estimates presented allow one to determine the discharge characteristics at the initial discharge. One electron emitted by the cathode initiates one runaway electron (and ion) avalanche in the gas gap, which produces some part of UV illumination from the drift space. As a result, $\kappa_v + \kappa_i$ new electrons, where $\kappa_i = \gamma_{i,a} K(d)$ is the current gain due to ion and fast atom bombardments of the cathode surface,¹⁴ will be emitted by the cathode. Then the current rise in the gap will be

$$\frac{d(\ln I_e)}{dt} = \frac{\kappa_v + \kappa_i - 1}{t^*}, \quad (7)$$

where t^* is the effective feedback time. If the mechanism is ionic, t^* is equal to a mean ion lifetime in the gap (it is ~ 5–20 ns in the experiments of Sec. 2). If the mechanism is photoelectric, t^* equals an UV luminescence time decay (~ 10 ns). For the numerical values of $\gamma_{i,a}$ from Ref. 14, $K(d)$ from Fig. 3b, and κ_v from Eq. (6), the numerical value of the right side of Eq. (7) can be calculated. The estimates obtained in such a way are in a good agreement with the time delay to a breakdown of a gas gap observed in experiments. It is the UV illumination whose effect on discharge dynamics at the first stage is predominant: $\kappa_v / \kappa_i = (2 - 3)/(0.3 - 0.5) = 6 - 8$.

On breakdown of the gap, when the e-beam current rises, the UV illumination flux sharply increases because some additional channels for gas excitation in the drift space appear. These are the generation of electrical fields there and the return current flowing along the e-beam-created plasma.¹⁸ The strength of this field near the anode is 20–100 V/cm for an e-beam current of 1 A and 200–400 V/cm for 10–20 A. This subject will be discussed in Sec. 4 more closely. The UV illumination from the e-beam-created plasma is more intense than that under direct excitation by an e-beam. Therefore, the temporal behavior of the UV illumination is determined by the electrical processes in the drift space and depends only indirectly on the discharge in the gap. Unfortunately, it seems very difficult to obtain currently quantitative evaluations of the UV illumination under these conditions. But clearly, that the role which the UV illumination plays in the discharge dynamics is no less than in the foregoing breakdown stage.

The short interelectrode gap. Owing to the short length of the interelectrode gap, all ionization processes in the gas are very weak. According to the data shown in Fig. 3, $K(d) = 0.1-0.5$ for typical conditions of the e-gun operation. The weakness of ionization does not allow a conventional glow discharge to be developed there. (Actually, the operating voltage applied to the e-gun is usually lower than the breakdown voltage of the gap without UV illumination.) Consequently, the short interelectrode distance determines the

discharge dynamics, its parameters, and the efficiency of e-beam production. We are coming now to their evaluations.

In a narrow gas gap with a strong external electric field ions quickly go out from the gas, i.e., the ion lifetime τ_i is short. Experiments^{1-3,15,16} show, that the condition $dI_e/dt \ll I_e/\tau_i$, where I_e is the e-beam current amplitude, holds over a wide range of gas pressures and cathode voltages. This means that the electric field distribution in the gap and the ion current follow the behavior of the e-beam current. The e-beam current is determined by the external (with respect to the gap) UV illumination and, therefore, it may be considered as a free parameter of the problem. The above-described circumstance allow one to use approximations which are typical of calculations of low-pressure gas-discharges e-guns.¹⁹ Neglecting ionization in the region of cathode-fall potential (an exact solution of this problem is beyond the scope of the paper), for a discharge in a narrow gas gap we obtain the following set of equations:

$$\bar{v}_i(x) = \Gamma \sqrt{E(x)/N}, \quad \Gamma = \sqrt{e/(2\sigma_{ex} M_i)}, \quad (8)$$

$$\frac{d^2 \varphi(x)}{dx^2} = \rho_i(x)/\epsilon_0, \quad \varphi(\delta) = \left. \frac{d\varphi(x)}{dx} \right|_{x=\delta} = 0, \quad (9)$$

$$j_i = \bar{v}_i \rho_i = \frac{j_e}{\theta_e} \int_{\delta}^d \left(-\frac{d\epsilon}{dx} \right)_e dx \approx j_e \frac{d-\delta}{1.7 J e U_d} \ln(BeU_d), \quad (10)$$

where $A = 1.3 \cdot 10^{-17} ZN$ in eV²/m and $B = 4/(15 Z^{4/3})$ in eV⁻¹ (see Ref. 17), \bar{v}_i is an average ion drift velocity in the region cathode-fall potential, σ_{ex} is the symmetric charge-exchange cross section, M_i is the ion mass, $\varphi(x)$ is the electric field potential at the distance x from the cathode, $\rho_i(x)$ is the ion density, ϵ_0 is the dielectric constant, δ is the size of the cathode-fall region, j_e is the electron current density at the cathode, $\theta_e = 1.7 J$ is the e-beam energy expended for one electron-ion pair production in the gas, and $(d-\delta)$ is the size of the plasma region in the gap. Notation of the remain values are given previously.

The set of Eqs. (8)–(10) yields the following solutions.

The potential distribution in the region of the strong field

$$\varphi(x) = U_d (1 - x/\delta)^{5/3}. \quad (11)$$

The maximum ion current density j_i , which is limited by the space-charge, is

$$j_i = 1.44 \varepsilon_0 \frac{\Gamma}{\sqrt{N}} \frac{U^{3/2}}{\delta^{3/2}}. \quad (12)$$

The equation for calculation of the width of the cathode-fall region δ current when the density in the e-beam j_e is known, has the form

$$\delta(d - \delta)^{0.4} = U_d \left[\frac{1.66 \cdot 10^6 \Gamma J}{Z j_e N^{3/2} \ln(BeU_d)} \right]^{0.4}. \quad (13)$$

Let us compare the estimates obtained from Eqs. (11)–(13) and the results of the experiments reported in Ref. 20, where the initial conditions are: the interelectrode gap is $d = 1.1$ mm, the neon pressure is 800 Pa ($Z = 10$, $J = 21.6$ eV, $N = 2 \cdot 10^{23}$ m⁻³, and $\Gamma = 3.16 \cdot 10^{12}$). Then Eq. (13) acquires the form

$$\delta(d - \delta)^{0.4} = U_d [1.27 \cdot 10^{-2} / j_e (2.52 + \ln U_d)]^{0.4}, \quad (14)$$

where δ and $(d - \delta)$ are measured in mm, j_e – in A/cm², and U_d – in kV. It has been established in Ref. 20 that when $j_e \geq 1$ kV and $j_e \geq 1$ A/cm² the cathode-fall region is between the cathode and probe No. 1, i.e., $\delta \leq 0.2$ mm. From Eq. (14) we obtain $\delta = 0.256$ mm assuming $U_d = U_{e/\max} = 2.4$ kV. By virtue of the profile (11) the value of the signal in probe No. 1 (see Ref. 20) is as low as 0.3 kV that is less than 1/8 of its initial value corresponding to the absence of ion space charges. The electric field distribution (11) agrees entirely with that measured in Ref. 20. Hence, we can be ascertained that Eqs. (11)–(13) adequately describe an actual discharge in the e-gun.

The efficiency of e-beam production can be represented as $\eta = j_e / (j_e + j_i) = (1 + j_i / j_e)^{-1}$, where the ratio j_i / j_e is calculated from Eq. (10) by substituting the value of δ obtained from Eq. (13). It follows herefrom that the thinner the plasma sheath in the gap, the higher is the efficiency of e-beam production in the discharge. But the thickness of the plasma sheath is determined appreciably by the length of the interelectrode gap. Therein lies the main effect of a short gas gap in the considered way of e-beam production.

The two important consequences following from Eqs. (8)–(14) should be noted. First, as follows from Eq. (13) the electric field strength at the cathode is lower for a shorter gas gap. This accounts for high discharge stability in short gas gaps. Second, calculations of δ from Eq. (13) for $d = 0.5$ mm and different U_d and N for helium and neon show that under optimal conditions for e-beam production there is no plasma sheath in the discharge gap and it is occupied entirely by the cathode-fall region (in this case Eqs. (13) and (14) have no solutions). Thus, the results of measurements performed in Ref. 20 for a gap at $d = 1.1$ mm, where actually $d \leq d/4$ is satisfied, give no way to state, as it is done in Ref. 20, that the e-beam is never generated until a very narrow cathode fall region at $\delta \ll d$ is formed.

In closing it should be noted that for $\delta \sim d$ the assumed approximation that disregards the ionization in the cathode fall region becomes ill-founded, and the problem should be solved in some other way.

4. USING THE RUNAWAY ELECTRON BEAMS FOR LASER PUMPING

The nanosecond range of e-beam pulse durations, the high peak power (up to 100 kW/cm²), and the ability to operate at high pulse repetition rates (up to 100–500 kHz) –

all these are attractive features of the above-described e-guns. The operating range of gas pressures is the same for the e-guns and for the cells of some types of lasers. Therefore, it is reasonable to use such e-beams for laser pumping. This was first done in 1981–1982 (see Refs. 21 and 22).

The energy deposition into a laser active medium by an e-beam differs dramatically from that produced by a pulsed electrical discharge. Indeed, when passing through the laser gas the e-beam generates secondary, tertiary, and so on electron avalanches. Therefore, the main part of the e-beam energy is expended for gas ionization: from ~50% in case of molecular gases and up to 60–70% in rare gases.²³ Only 4–6% of the total e-beam energy is expended for excitation of vibrational states while the bulk of the remaining energy – for direct excitation of electron levels.²⁴ The electron energy distribution in the e-beam created plasma is described by a degradation spectrum,¹⁷ which is determined by the sort of the buffer gas for a metal vapor laser.²⁵ The degradation occurs for a time close to that required for fast electrons to pass over the active medium of the laser, i.e., for about 1–10 ns. The energy density contributed by an e-beam in a gas is described by the Bethe-Miller formula

$$\frac{d\varepsilon}{dx} = \frac{4\pi e^4}{m_e v_e} NZ \ln \left(\frac{2 m_e v_e^2}{15 Z^{4/3}} \right), \quad (15)$$

and the mean free path of the e-beam electrons is given by

$$l(\varepsilon) \approx m_e^2 v_e^4 / (16\pi e^4 ZN) [\ln(2 m_e v_e^2 / 15 Z^{4/3})]^{-1} \quad (16)$$

The forms of these formulas suitable for practical calculations are the following:

$$\frac{d\varepsilon}{dx} \left(\frac{\text{eV}}{\text{cm}} \right) = \frac{1.3 \cdot 10^{-16}}{\varepsilon} ZN [5.59 + \ln \varepsilon \ln Z - 1.33 \ln Z], \quad (15a)$$

$$l \approx \frac{3.84 \cdot 10^{18} \varepsilon^2}{ZN} / [5.59 + \ln \varepsilon - 1.33 \ln Z], \quad (16a)$$

where the quantities involved must be expressed in the following units: N in cm⁻³, ε in keV, and l in cm. Then $d\varepsilon/dx$ will be obtained in eV/cm.

Experiments with metal vapor lasers pumped by both runaway electron beams and pulsed electrical discharges performed by Bokhan²⁶ have demonstrated the great advantages of the e-beams in producing high power laser emission with a higher efficiency. Thus, in Ref. 6 it has been shown that the optimum of the pulse repetition rate in Pb and Mn lasers pumped by e-beams exceeds 80 kHz, i.e., by a factor of magnitude 10–15 greater than that obtained with discharge pumping. The physical efficiency of these lasers estimated from the e-beam energy deposited into the active medium was an order of magnitude higher too. The output power of 120 and 60 W has been achieved for lasing in Mn and Pb vapors, respectively, when a 50 kW high frequency power supply operating in a regime of long pulse trains was used. These results are two orders of magnitude larger than those obtained with pulsed discharge pumping. Using the e-beam excitation technique, quasicontinuous laser oscillations with highly reduced parameters have been produced by some transitions of atoms and ions.^{26,27}

A realization in practice of the e-beam pumping depends on the geometry of e-beam injection into the active zone of the laser. In general only radial and longitudinal arrangements of pumping are applicable in metal vapor lasers. Let us discuss two versions of arrangements in details.

Radial pumping. As the energy of electrons in the beams 1 obtained in the first experiments was no more than 3–5 keV, only transverse geometry of the e-beam injection could then be used. As applied to metal vapor lasers this means that the e-gun should be placed inside the heated zone of the laser cell. The e-gun design with a hollow-cathode and hollow-anode geometry²⁸ shown in Fig. 5a is capable of operating under these conditions solely. This design was used by Bokhan in his experiments. Laser cells with the e-guns of inner diameter 0.5–3 cm and up to 100 cm long having the 0.2–0.5 mm distance between the cathode and the anode were constructed. These devices were capable of operating at temperatures up to 1300°C (see Ref. 26). Testing however, has shown that this geometry requires some special measures to be taken to produce e-beams with good parameters. It turned out that the applied voltage at the metal–cathode gun cannot be higher than 3–3.5 kV because of sparking and arcing developing at higher voltages. Therefore, the produced e-beam current densities are low. Thus, for the pulse repetition rate $f = 20$ kHz the average e-beam power reduced to the cathode area was no more than 2.5 W/cm². This is far below the results obtained with the help of planar e-guns. This low operating voltage leads to low efficiency of e-beam production (see Fig. 4). This problem was solved by using some resistive and percolating materials for the cathode. This allows one to raise the voltage up to 6–7 kV and increase the reduced e-beam energy down to 3 mJ/cm² per pulse ($j_e = 11$ A/cm²) with an Al₂O₃ cathode and up to 12 mJ/cm² per pulse ($J_e = 44$ A/cm²) with a percolating cathode. Finally, e-beam pulses with an energy of 11.5 J per pulse are produced with the percolating–cathode e-gun 3 cm in diameter and 100 cm long operating at $f = 1$ Hz and a temperature of 20°C. This remarkable result demonstrates the possibilities of the e-beam production technique.

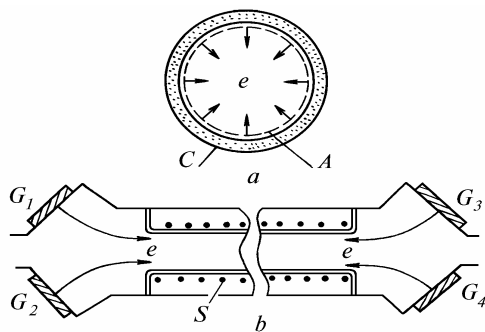


FIG. 5. Schematic diagrams of the lasers pumped by runaway electron beams: radial (a) and longitudinal (b) geometries. A is the anode and C is the cathode of the e-gun, S is the pulsed magnetic coil, and G_{1–4} are die e-guns.

The experiments show that some engineering, technical, and physical problems must be solved prior to creating metal vapor lasers pumped by the radial e-guns. The most complicated engineering problem is the choice of the ceramic material for the e-gun cathode which possesses a required electrical conductivity in the given range of temperatures and be resistive to cracking under the action of high current pulses passing through it. The technical problems are connected first of all with fast switching of 3–50 kA currents at repetition rates of 1–10 kHz and higher. The problem remains unsolved yet. Therefore it is the conventional switch employed now (such as hydrogen thyatrons, high current modulating tubes, and spark gaps)

that determines the operating regime of the e-gun and output laser parameters.

A very serious problem is the reduction of the efficiency of e-beam production in the radial geometry in comparison with that achieved in the planar geometry (see Sec. 2). The physical nature of this effect is as follows. In reality, the active medium of a laser is rather transparent for a 4–6 keV e-beam propagating in a radial direction. The fast electrons of the beam passing through the active space come into the discharge space again from the opposite side, decelerate there in the opposing strong electric field, turn back, accelerate again and finally withdraw from the space. During their flight the electrons ionize the gas and doing so they increase the ion current in the discharge space (see Sec. 3). As the fast electrons have only the n th fraction of the initial energy of the beam electrons, according to Eq. (15) their ionizing power per unit length is n^{n-1} times higher. Consequently, in the approximation used to derive Eqs. (8)–(14) the ion current in the radial e-gun is $(1 + 2/n)$ times greater than that in the planar. Therefore, if η_0 is the efficiency of the e-beam production in the planar e-gun ($\eta_0 = (1 + j_i / j_e)^{-1}$) and hence $j_i / j_e = (1 - \eta_0) / \eta_0$, then the efficiency of a radial e-gun

$$\eta_r = \frac{\eta_0}{1 + 2(1 - \eta_0)/n}. \quad (17)$$

So, suppose that a planar e-gun is filled with helium at a density $N = 1 \cdot 10^{18}$ cm⁻³ and generates a 4 keV e-beam with an efficiency $\eta_0 = 0.7$. Then for the radial e-gun 3 cm in diameter with other parameters being the same the efficiency η_r is equal to 0.36 (because from Eq. (15) we have $(d\epsilon/dx)_e = 0.4$ keV/cm and $n = 0.65$), that is about a half of that for the planar. This situation cannot be tolerable for actual laser devices, therefore it is necessary to provide a complete retardation of the initial e-beam in the active space inside the anode.

The described effect is probably the main reason for the low voltage threshold for appearance of some sorts of discharge instabilities in the radial geometry in comparison with the planar one, which were mentioned above.

Longitudinal pumping. In this case the e-gun (one or more) is placed in the cold zone of the laser cell, and the e-beam is compressed, turned and guided along the heated operating zone (see Fig. 5b). Hence, there is a freedom to choose the structural materials for the gun, its dimensions, geometry, etc. There appears the possibility to simplify extremely the e-gun design and replace the e-guns without disassembling the laser cell. But in this case a special magnet system is needed to control the e-beam, and some limitations on the rate of energy input into the operating laser zone appear. At first consider some issues of fundamental importance.

It is known that a significant electric field may be induced in a long e-beam-sustained plasma filament.^{18,29} Such a field is capable of not only hindering appreciably the e-beam propagation but also of preventing the e-beam from entering the narrow laser cell at all. This circumstance is quite essential for the runaway electron beams, because they have rather low kinetic energies (less than 10 keV). One of the retarding potential components is associated with the inductance of the e-beam-sustained plasma filament: $\Phi_{RL} = -L(dI_e/dt)$, where L is the inductance and dI_e/dt is the rise rate of the e-beam current. For a coaxial geometry of the filament and the return current busbar which surrounds the laser cell, the following relation can be obtained:

$$\frac{\varphi_{RL}}{l_f} = \frac{\mu_0}{2\pi} \ln \left(\frac{D_b}{D_f} \right) \frac{dI_e}{dt}, \quad (18)$$

where D_f and D_b are the diameters of the filament and the busbar, respectively; l is the filament length, and μ_0 is the magnetic permittivity of vacuum. If $D_b/D_f = 3$ and $dI_e/dt = 1 \cdot 10^{10}$ A/s then $\varphi_{RL}/l_f = 2$ kV/m.

The second component of the space potential is an electrostatic potential appearing because of incomplete e-beam-charge neutralization in the filament. A simple calculation shows that the potential of an e-beam plasma filament grounded on its ends is maximum at the middle of the length l and for $l_f \gg D_f$ it is defined as

$$\varphi_{Re} = 9 \cdot 10^9 \frac{\Delta Q_f}{l_f} (0.5 + \ln(2 l_f/D_f)), \quad (19)$$

where ΔQ_f is the unneutralized charge of the filament. Therefore, at $D_e = 1$ cm, $l_f = 0.5$ m, $I_e = 100$ A, and for the 1% charge unneutralization we have $\varphi_{Re} = 1$ kV.

The relations show that any attempts to realize longitudinal pumping by rarely repeated runaway electron beam pulses having a current more than 1 kA and risetime less than 10 ns are doomed to failure as it has been obtained in Ref. 30. However, a laser containing two e-guns (each of them being at every end of the laser cell), each producing 10 keV e-beam pulses of current 500 A, risetime 25 ns, and duration 60 ns can be run properly. Such a laser having a 1-m long operating zone and a grounded cylindrical electrode in the middle provides 0.5 J pumping pulses. For a pulse repetition rate of 50 kHz the average pumping power reaches 25 kW. Note that the available standard switches are capable of providing the laser operation in such a regime. It must be stressed that the retarding potential decreases essentially, when a high repetition rate regime of e-gun operation is used, due to high conductivity of the plasma filament.

Of technical problems most important are those associated with search for and optimization of the magnetic system for controlling the e-beam. Several variants of the system have been examined in Ref. 18 and an efficient way is found for uniting the e-beams from several e-guns with the help of a singly pulsed thin solenoid (its diameter being only 2–4 times larger than that of the filament). The magnetic-field strength in the solenoid must be in the range 70–100 kA/m. However, the fact that the solenoid is placed in the heated zone of the laser operating at temperatures higher than 1700°C gives rise to the problem concerning the energy dissipation by the solenoid, as the most suitable material for it is molybdenum, which, however, has too low conductivity in this case. Actually, the electrical power dissipated by the solenoid winding is described by the relation:

$$\overline{W}_s = (\pi/2 \kappa) \rho_T (1 + D/h) H^2 l_s, \quad (20)$$

where ρ_T is the resistivity of the winding's material at operating temperature (for molybdenum $\rho_T = 4.2 \cdot 10^{-7} \Omega \cdot m$ at 1700°C), D , h , and κ are the diameter, thickness, and space factor of the winding, l_s is the solenoid length, and H is the magnetic-field strength. Therefore, $W_s/l_s = (10/\kappa)$ kW/m and $H = 70$ kA/m at 1700°C. For obviously, such a laser can operate only in a regime of pulse trains repeated with the off-duty factor more than 5–10, otherwise other variants of e-beam control systems must be used. The longitudinal laser pumping by runaway electron beams is currently realized

for only the metal vapors zinc and cadmium having low operating temperatures.¹⁸

CONCLUSION

The analysis of the data shows that the discharge in a short interelectrode gap generating a runaway electron beam with an efficiency $\sim 50\%$ and more differs essentially from the well-known glow discharges. The dynamics of this type of discharge and its I-V characteristics are affected strongly by the processes taking place in the drift space behind the e-gun anode. The cathode-fall region of the discharge is abnormally large and, probably, it has no time at all to be formed during the e-beam generation. The relations which connect the size of the cathode-fall region with the discharge gap parameters, the e-beam current, and the cathode voltage are derived.

The longitudinal and radial geometries of the e-beam pumping of metal-vapor lasers are analyzed. It is shown that in all previous experiments where radial e-guns were used for metal-vapor laser pumping, the efficiency of the e-beam production was significantly lower than in the planar e-guns. The reason is too low retarding capability of the active laser media. For the geometry of the longitudinal laser pumping some limitations on the rate of the e-beam energy input into the heated zone have been disclosed and the way for overcoming them is briefly outlined.

The results of the analyses performed in this paper are expected to be useful in further theoretical and practical works.

REFERENCES

1. P.A. Bokhan and G.V. Kolbychev, *Pis'ma Zh. Tekh. Fiz.* **6**, No. 7, 418–421 (1980).
2. P.A. Bokhan and G.V. Kolbychev, *Zh. Tekh. Fiz.* **51**, No. 9, 1823–1831 (1981).
3. G.V. Kolbychev and E.A. Samyshkin, *Zh. Tekh. Fiz.* **51**, No. 10, 2032–2037 (1981).
4. G.V. Kolbychev and I.V. Ptashnik, in: *Proceeding of the 3rd All-Union Conference on Physics of Gas Discharges*, Kiev (1986), Part. 3, pp. 366–368.
5. P.A. Bokhan, *Pis'ma Zh. Eksp. Teor. Fiz.* **42**, No. 8, 335–337 (1985).
6. P.A. Bokhan, *Kvant. Elektron.* **13**, No. 9, 1837–1847 (1986).
7. G.A. Mesyats, Yu.I. Bychkov, and V.V. Kremnev, *Usp. Fiz. Nauk* **107**, No. 2, 201–228 (1972).
8. A.I. Pavlovskii, L.P. Babich, T.V. Loiko, and L.V. Tarasova, *Dokl. Akad. Nauk SSSR* **281**, No. 6, 1359–1363 (1985).
9. E.D. Lozanskii and O.B. Firsov, *Theory of Spark* (Atomizdat, Moscow, 1975), 272 pp.
10. T.V. Loiko, L.V. Tarasova, and V.A. Tsukerman, *Pis'ma Zh. Tekh. Fiz.* **3**, No. 3, 120–122 (1977).
11. G.V. Kolbychev, "Study of the electron runaway phenomenon in medium-pressure gas", Ph. Cand. Dissert. Phys.–Math. Sc., Institute of Atmospheric Optics, Siberian Branch of the Academy of Sciences of the USSR, Tomsk (1983).
12. G.V. Kolbychev, in: *Contributed Papers of 15m International Conference on Phenomena in Ionized Gases*, Minsk (1981), Pt. II, pp. 619–620.
13. G.D. Alkhazov, *Zh. Tekh. Fiz.* **44**, No. 5, 1044–1046 (1974).
14. K.N. Ulyanov and V.V. Chulkov, *Zh. Tekh. Fiz.* **58**, No. 2, 328–334 (1988).
15. G.V. Kolbychev and I.V. Ptashnik, *Pis'ma Zh. Tekh. Fiz.* **11**, No. 18, 1106–1110 (1985).
16. G.V. Kolbychev and I.V. Ptashnik, *Zh. Tekh. Fiz.* **59**, No. 9, 104–111 (1989).

17. Gudzenko and S.I. Yakovlenko, *Plasma Lasers* (Atomizdat, Moscow, 1978), 256 pp.
18. G.V. Kolbychev, P.D. Kolbycheva, and O.B. Zabudskii, *Atmos. Oceanic Opt.* **6**, No. 3, 153–156 (1993).
19. K.N. Ulyanov and Ya.I. Lender, *Teplofiz. Vysokikh Temp.* **17**, No. 5, 949–959 (1979).
20. P.A. Bokhan, *Zh. Tekh. Fiz.* **61**, No. 6, 61–68 (1991).
21. G.V. Kolbychev and E.A. Samyshkin, *Kvant. Elektron.* **10**, No. 2, 437–438 (1983).
22. P.A. Bokhan and A.R. Sorokin, *Pis'ma Zh. Tekh. Fiz.* **8**, No. 15, 947–950 (1982).
23. V.N. Kondrat'ev and E.E. Nikitin, *Kinetics and Mechanisms of Gas-Phase Reactions* (Nauka, Moscow, 1975), 559 pp.
24. V.P. Kononov and E.E. Son, *Zh. Tekh. Fiz.* **50**, No. 2, 300–306 (1980).
25. B.L. Borovich, V.V. Buchanov, and E.I. Molodykh, *Kvant. Elektron.* **11**, No. 5, 1005–1014 (1984).
26. P.A. Bokhan, "*Metal vapor lasers with collisional deexcitation of low operating levels*", Author's Abstract of Doct. Phys.—Math. Sci. Dissert., Institute of Atmospheric Optics and Institute of Thermophysics, (both) Siberian Branch of the Academy of Sciences of the USSR, Tomsk, Novosibirsk (1988).
27. P.A. Bokhan, *Kvant. Elektron.* **13**, No. 8, 1595–1602 (1986).
28. K. Rozsa, M. Janossy, L. Scillag, and J. Bergou, *Opt. Commun.* **23**, No. 2, 162–164 (1977).
29. G. Wallis, K. Zauer, D. Zunder, et al., *Usp. Fiz. Nauk* **113**, No. 3, 435–462 (1974).
30. P.A. Bokhan and A.R. Sorokin, *Zh. Tekh. Fiz.* **61**, No. 7, 187–190 (1991).